CHAPTER 3

AN IN-DEPTH INVESTIGATION ON PLANE HARMONIC WAVES UNDER TWO-TEMPERATURE THERMOELASTICITY WITH TWO RELAXATION PARAMETERS[1]

3.1 Introduction

In previous chapter, we have investigated one problem in the context of two-temperature thermoelasticity theory that includes two thermal relaxation parameters. We have highlighted some characteristic features of the model based on thermoelastic interactions due to thermal shock applied at the stress free boundary of a cylindrical cavity inside a thermoelastic medium. In this chapter, we are going to discuss the harmonic plane wave propagation in this two-temperature thermoelasticity theory.

It is worth to be mentioned that several researchers have tried to interpret the propagation of harmonic plane waves in an elastic medium. The propagation of plane waves in classical thermoelasticity was studied by Chadwick and Sneddon (1958) and Chadwick (1960). The propagation of plane waves in the generalized thermoelasticity which has one relaxation time is discussed by Nayfeh and Nemat-Nasser (1971) and afterward by Puri (1973). Subsequently, Agarwal (1979) has given the details of

[1]The content of this chapter is published in ***"Mathematics and Mechanics of Solids"*, 22 (2), (2017), 191-209.**

the propagation of plane waves in the generalized thermoelasticity which has one relaxation time. Haddow and Wegner (1996) reviewed again the wave propagation in Green-Lindsay model and Lord-Shulman model. The order of magnitude of thermal relaxation time in Green-Lindsay model was found by Suh and Burger (1998). Interpretation on plane waves in the reference of thermoelasticity of Green-Naghdi of type-II is noted by Chandrashekharaiah (1996). Puri and Jordan (2004) and Kothari and Mukhopadhyay (2012) investigated the propagation of plane waves in type-III thermoelastic medium.

The objective of the current chapter is to interpret the propagation of plane harmonic waves in a homogeneous and isotropic unbounded medium in the reference of the linear theory of two-temperature thermoelasticity with two relaxation parameters (TGL). The propagation of plane waves in a thermoelastic medium has been investigated earlier by Kumar and Mukhopadhyay (2010b) for two-temperature thermoelasticity with one thermal relaxation parameter (TLS). Being motivated by the results as found out in (Kumar *et al.* (2016)), we have made an attempt to extend the work of Puri and Jordan (2006) and Kumar and Mukhopadhyay (2010b) and investigate the effects of two thermal relaxation time parameters on plane harmonic wave under two-temperature theory for the purpose of comparing the results predicted by TGL model with the corresponding results of TLS, LS and GL models. For this, we formulate the problem in the context of four models of thermoelasticity, namely: thermoelasticity with one relaxation parameter (LS model), thermoelasticity two thermal relaxation parameters (GL model), two-temperature thermoelasticity with one relax-

ation parameter (TLS) and the two-temperature thermoelasticity with two relaxation parameters (TGL model) in a unified way. After mathematical formulation of the present problem, we obtain the dispersion relation solutions of longitudinal plane waves. We find the asymptotic expansions of several qualitative characterizations of the wave field, such as, phase velocity, specific loss and penetration depth for the high and low frequency values for this model. In order to verify these analytical results predicting the limiting behavior of the wave characteristics, numerical values of the above mentioned quantities for intermediate values of frequency are also computed directly by applying computational tool. Finally, we analyze the results in a detailed way by comparing our analytical as well as numerical results with the corresponding results of all four models as mentioned.

3.2 Basic Governing Equations

We consider an unbounded, isotropic and thermally conducting elastic medium characterized by the density, ρ and the Lame's elastic constants- λ, μ. The dynamic displacement vector is measured from a steady state position and the deformation is supposed to be very small. Therefore, the constituent equations and basic governing equations for the thermoelastic interactions inside the medium in absence of body forces and heat sources in the contexts of four models: the LS, GL, TLS and TGL models in a unified way can be written as follows:

Stress-strain temperature relation:

It gives the relation between stress, strain and the inducing temperature and is given by the relation

$$\sigma_{ij} = \lambda e\delta_{ij} + 2\mu e_{ij} - \gamma(\theta + \tau_1 \frac{\partial \theta}{\partial t})\delta_{ij} \tag{3.1}$$

Strain-displacement relation:

$$e_{ij} = \frac{1}{2}(u_{i,j} + u_{j,i}) \tag{3.2}$$

Heat conduction equation without heat source:

$$K\phi_{,ii} = \rho c_E(\frac{\partial \theta}{\partial t} + \tau_0 \frac{\partial^2 \theta}{\partial t^2}) + \gamma\theta_0(\frac{\partial e}{\partial t} + \tau_0 \xi \frac{\partial^2 e}{\partial t^2}) \tag{3.3}$$

Equation of motion without body force:

Equation of motion as derived by Newton's law of motion and without any body force is given by the following equation:

$$\sigma_{ij,j} = \rho \ddot{u}_i \tag{3.4}$$

The thermodynamic temperature, θ is related to the conductive temperature, ϕ by the following relation (Chen and Gurtin, 1968):

$$\phi - \theta = \alpha\phi_{,ii} \tag{3.5}$$

where $\alpha \geq 0$ is the two-temperature parameter for two-temperature thermoelasticity theory.

The above set of equations (3.1)-(3.5) reduce to the corresponding equa-

tions under four different models as mentioned above with different values of the parameters $\xi,\ \alpha$ and the thermal relaxation time parameters τ_0 and $\tau_1$as follows:

- **TGL Model:** $\xi = 0,\ \alpha \neq 0,\ \tau_0 \neq 0,\ \tau_1 \neq 0$
- **TLS Model:** $\xi = 1,\ \alpha \neq 0,\ \tau_0 \neq 0,\ \tau_1 = 0$
- **GL Model:** $\xi = 0,\ \alpha = 0,\ \tau_0 \neq 0,\ \tau_1 \neq 0$
- **LS Model:** $\xi = 1,\ \alpha = 0,\ \tau_0 \neq 0,\ \tau_1 = 0$

3.3 Problem Formulation

Since we considered an unbounded isotropic and homogeneous thermoelastic medium, we assume, without any loss in generality, that the plane wave is propagating in the medium in the x_1 direction and suppose all field variables depends on x_1 (now denote as x) and t only.

Hence, using equations (3.1), (3.2) and (3.5), the equation of motion (3.4) can be written in the form

$$(\lambda + 2\mu)\frac{\partial^2 u}{\partial x^2} - \gamma\frac{\partial}{\partial x}[(\phi - \alpha\frac{\partial^2 \phi}{\partial x^2}) + \tau_1\frac{\partial}{\partial t}(\phi - \alpha\frac{\partial^2 \phi}{\partial x^2})] = \rho\frac{\partial^2 u}{\partial t^2} \qquad (3.6)$$

Combining equations (3.3) and (3.5), we get

$$[K + \alpha\rho c_{_E}(\frac{\partial}{\partial t} + \tau_0\frac{\partial^2}{\partial t^2})]\frac{\partial^2 \phi}{\partial x^2} = \rho c_E(\frac{\partial}{\partial t} + \tau_0\frac{\partial^2}{\partial t^2})\phi + \gamma\theta_0(\frac{\partial}{\partial t} + \tau_0\xi\frac{\partial^2}{\partial t^2})e \quad (3.7)$$

To make the equations (3.6) and (3.7) simpler, we use the following

dimensionless transformations:

$x' = c_0\eta x,\ u' = c_0\eta u, \tau_0' = c_0^2\eta\tau_0,\ \tau_1' = c_0^2\eta\tau_1,\ t' = c_0^2\eta t,\ \theta' = \frac{\theta-\theta_0}{\theta_0},$ $\eta = \frac{\rho c_E}{K},\ \phi' = \frac{\phi-\theta_0}{\theta_0},\ e' = e,\ c_0^2 = \frac{\lambda+2\mu}{\rho},\ \beta_1 = \frac{\gamma\theta}{\lambda+2\mu},\ \beta_2 = \frac{\gamma}{K\eta},\ \alpha' = ac_0\eta^2.$

Now, after dropping the primes for convenience, equations (3.6) and (3.7) reduce to the following forms:

$$\frac{\partial^2 u}{\partial x^2} - \beta_1\frac{\partial}{\partial x}[(\phi - \alpha'\frac{\partial^2\phi}{\partial x^2}) + \tau_1\frac{\partial}{\partial t}(\phi - \alpha'\frac{\partial^2\phi}{\partial x^2})] = \frac{\partial^2 u}{\partial t^2} \tag{3.8}$$

$$[1 + \alpha'(\frac{\partial}{\partial t} + \tau_0\frac{\partial^2}{\partial t^2})]\frac{\partial^2\phi}{\partial x^2} = (\frac{\partial}{\partial t} + \tau_0\frac{\partial^2}{\partial t^2})\phi + \beta_2(\frac{\partial}{\partial t} + \tau_0\xi\frac{\partial^2}{\partial t^2})e \tag{3.9}$$

3.4 Dispersion Equation

We find that the shear wave remains uncoupled with the thermal field, whereas, in case of dilatation wave, the mechanical and thermal fields are coupled together. So we will concentrate on the longitudinal wave only and we consider the solution of Eqns. (3.8) and (3.9) for the longitudinal plane wave in the forms

$$u = Ae^{i(\omega t - \gamma x)} \tag{3.10}$$

$$\phi = Be^{i(\omega t - \gamma x)} \tag{3.11}$$

where ω is a positive real number and γ is a complex constant. A and B are complex amplitudes (simultaneously not both zero). Phase velocity of wave is therefore given by $\frac{\omega}{\text{Real}(\gamma)}$, that adapt to the longitudinal waves for

which frequency and wavelength are $\frac{\omega}{2\pi}$ and $\frac{2\pi}{\text{Real}(\gamma)}$, respectively. $\text{Real}(\gamma) > 0$ and $\text{Im}(\gamma) \leq 0$ must hold obviously for the wave to be realistic.

Now, substituting (3.10) and (3.11) into equations (3.8) and (3.9), we obtain

$$\begin{bmatrix} \omega^2 - \gamma^2 & -\beta_1(\tau_1\omega\gamma + \tau_1\alpha'\omega\gamma^3) + i\beta_1(\gamma + \alpha'\gamma^3) \\ \beta_2(\omega\gamma + i\tau_0\xi\omega^2\gamma) & (\gamma^2 - \tau_0\alpha'\omega^2\gamma^2 - \tau_0\omega^2) + i(\omega + \alpha'\omega\gamma^2) \end{bmatrix} \begin{bmatrix} A \\ B \end{bmatrix} = \begin{bmatrix} 0 \\ 0 \end{bmatrix} \tag{3.12}$$

Obviously, for non-trivial solution of the system of equations (3.12), the determinant of the above system must be zero. Therefore, we obtain

$$\begin{aligned} &[(-1 + \tau_0\alpha'\omega^2 + h\tau_1\alpha'\omega^2 + h\tau_0\alpha'\xi\omega^2) + i(-\epsilon\alpha'\omega + h\tau_0\tau_1\alpha'\xi\omega^3)]\gamma^4 \\ &+[(\omega^2 - \tau_0\alpha'\omega^4 + \tau_0\omega^2 + h\tau_1\omega^2 + h\tau_0\xi\omega^2) + i(\alpha'\omega^2 - \epsilon\omega + h\tau_0\tau_1\xi\omega^3)]\gamma^2 \\ &+(-\tau_0\omega^4 + i\omega^3) = 0 \end{aligned} \tag{3.13}$$

where $h = \beta_1\beta_2$, and $\epsilon = 1 + h$.

Equation (3.13) represents a unified dispersion relation for the above system in the contexts of four models. Now, we are interested in the case in which $\xi = 0, \alpha \neq 0, \tau_0 \neq 0, \tau_1 \neq 0$. This case corresponds to the TGL case. Thus putting $\xi = 0$, equation (3.13) changes to the following form:

$$\begin{aligned} &[(-1 + \tau_0\alpha'\omega^2 + h\tau_1\alpha'\omega^2) - i\epsilon\alpha'\omega]\gamma^4 + [(\omega^2 - \tau_0\alpha'\omega^4 + \tau_0\omega^2 + h\tau_1\omega^2) \\ &+i(\alpha'\omega^2 - \epsilon\omega)]\gamma^2 + (-\tau_0\omega^4 + i\omega^3) = 0 \end{aligned} \tag{3.14}$$

Finally taking $\gamma = Z\sqrt{\omega}$ and making coefficient of Z^4 real, we get

$$A(\omega)Z^4 + (P - iQ)Z^2 + (U + iV) = 0 \tag{3.15}$$

where

$A(\omega) = a_1\omega^4 + a_2\omega^2 + 1$, $P = -p_1\omega^5 - p_2\omega^3 - p_3\omega$, $Q = -q_1\omega^4 - q_2\omega^2 - \epsilon$, $U = -u_1\omega^4 - u_2\omega^2$, $V = v_1\omega^3 - \omega$,

and

$a_1 = \tau_0^2\alpha'^2 + \tau_1^2\alpha'^2h^2 + 2\tau_0\tau_1\alpha'^2h$, $a_2 = \epsilon^2\alpha'^2 - 2\tau_0\alpha' - 2\tau_1\alpha'h$, $p_1 = \tau_0^2\alpha'^2 + \tau_0\tau_1\alpha'^2h$, $p_2 = -(2\tau_0\alpha' + \tau_0^2\alpha' + 2\tau_0\tau_1\alpha'h + \tau_1\alpha h + \tau_1^2\alpha'h^2 - \alpha'^2\epsilon)$,

$p_3 = 1 + \tau_0 + \tau_1h - \alpha\epsilon^2$,

$q_1 = \alpha'^2h(\tau_1 - \tau_0)$, $q_2 = \alpha'h$, $u_1 = (\tau_0^2\alpha' + 2\tau_0\tau_1\alpha'h)$, $u_2 = -\tau_0 + \alpha'\epsilon$,

$v_1 = \tau_0\alpha' + \tau_1\alpha h - \tau_0\alpha'\epsilon$.

Equation (3.14) is therefore the dispersion relation for the TGL model and it clearly incorporate the effects of the two thermal relaxation parameters and the two-temperature parameter on the longitudinal plane wave. This dispersion relation reduces to the dispersion relation under GL model when $\alpha = 0$. The dispersion relations for the TLS model and the LS model can be obtained as special cases from equation (3.13) by assuming corresponding values of $\xi, \alpha, \tau_0, \tau_1$as mentioned in section 2.

3.5 Solution of Dispersion Relation under TGL Model

If roots of the equation (3.15) are $\pm Z_1$, and $\pm Z_2$, then we can write

$$Z_{1,2}^2 = \frac{-(P - iQ) \pm \sqrt{D(\omega)}}{2A(\omega)} \tag{3.16}$$

where,

$$Real(D(\omega)) = p_1^2\omega^{10} + N_1\omega^8 + N_2\omega^6 + N_3\omega^4 + N_4\omega^2 - \epsilon^2.$$

$$Im(D(\omega)) = 2p_1q_1\omega^9 - M_1\omega^7 - M_2\omega^5 + M_3\omega^3 + M_4\omega.$$

with,

$N_1 = 2p_1p_2 - q_1^2 + 4a_1u_1$, $N_2 = p_2^2 + 2p_3p_1 - 2q_1q_2 + 4a_1u_2 + 4a_2u_1$,

$N_3 = 2p_2p_3 - q_2^2 - 2\epsilon q_1 + 4a_2u_2 + 4u_1$, $N_4 = p_3^2 - 2\epsilon q_2 + 4u_2$,

$M_1 = 2p_1q_2 + 2p_2q_1 + 4a_1v_1$, $M_2 = 2p_3q_1 + 2\epsilon p_1 + 2p_2q_2 - 4a_1 + 4a_2v_1$,

$M_3 = -(2p_3q_2 + 2\epsilon p_2 - 4a_2 + 4v_1)$, $M_4 = -2\epsilon p_3 + 4$.

Equation (3.16) can be solved by applying the following theorem of complex numbers:

Theorem: (Ponnusamy (2005)) : For a given $z = x + iy \; \epsilon \; \mathbb{C}$, the solutions of $w^2 = z$ are given by

$$w = \left[\sqrt{\frac{|z| + x}{2}} + i\, sgn(y)\sqrt{\frac{|z| - x}{2}}\right],\ where,\ sgn(y) = \begin{cases} +1 & if\ y \geq 0 \\ -1 & if\ y < 0 \end{cases}$$

Using above theorem in Eqn. (3.16), we can find two values of Z and therefore γ, whose imaginary parts are negative. These two values of γ correspond to two types of the dilatation waves in which first one is predominantly elastic wave and second one is thermal wave in nature. We denote γ related with the first one by γ_1 and the second one by γ_2.

3.6 Analytical Results

Since the general analysis of waves on the basis of the roots given by (3.16) is highly complicated, we therefore concentrate on the analysis of wave and the effects on thermal relaxation parameter and the two-temperature parameter under two special cases which correspond to the waves of very high and very low frequency. Hence, we first obtain the expressions for Z_1 and Z_2 from equation (3.16) by applying above theorem under these two special cases by assuming ω to be very large and very small, respectively. Therefore, we proceed as follows:

3.6.1 Case-I: High frequency asymptotic expansions

In this case, we assume that ω to be very large, i.e., $\omega \ggg 1$. Hence, expanding equation (3.16) for large ω and neglecting higher powers of $\frac{1}{\omega}$ we write equation (3.16) as

$$Z_{1,2}^2 = \frac{-(P - iQ) \pm (S - iT)}{2A(\omega)}$$

where

$$S = p_1\omega^5 + \frac{K_1}{2p_1}\omega^3 + \left(\frac{K_2}{2p_1} - \frac{K_1^2}{8p_1^3}\right)\omega + \left(\frac{K_3}{2p_1} - \frac{K_1K_2}{4p_1^3}\right)\frac{1}{\omega} + o(\frac{1}{\omega^2}.)$$

and

$$T = \sqrt{L_1}\omega^4 + \frac{L_2}{2\sqrt{L_1}}\omega^2 + \left(\frac{L_3}{2\sqrt{L_1}} - \frac{L_2^2}{8L_1^{3/2}}\right) + o(\frac{1}{\omega^2}.)$$

where

$K_1 = \frac{N_1}{2} + \frac{m_1}{4p_1^2}$, $K_2 = \frac{N_2}{2} + \frac{m_2}{4p_1^2} - \frac{m_1^2}{16p_1^6}$, $L_1 = \frac{m_1}{4p_1^2} - \frac{N_1}{2} = q_1^2$, $L_2 = -\frac{N_2}{2} + \frac{m_2}{4p_1^2} - \frac{m_1^2}{16p_1^6}$, $m_1 = 2N_1p_1^2 + 4p_1^2q_1^2$, $m_2 = 2N_2p_1^2 + N_1^2 + 4p_1q_1M_1$,

3.6.2 Analytical results for $\gamma_{1,2}$

By expanding above equation for $Z_{1,2}^2$ for large ω and neglecting higher powers of $\frac{1}{\omega}$ we carry out detailed manipulations and obtain

$$Z_{1,2}^2 = X_{1,2} + iY_{1,2},$$

where

$$X_1 = -\frac{A_1}{\omega} - \frac{A_2}{\omega^3} + o(\frac{1}{\omega^5})$$

$$Y_1 = -\frac{B_1}{\omega^2} + \frac{B_2}{\omega^4} + o(\frac{1}{\omega^6})$$

$$X_2 = C_1\omega + \frac{C_2}{\omega} + o(\frac{1}{\omega^3})$$

$$Y_2 = -D_1 - \frac{D_2}{\omega^2} + o(\frac{1}{\omega^4})$$

with

$A_1 = \frac{1}{2a_1}\left(\frac{K_1}{2p_1} - p_2\right)$, $A_2 = \frac{1}{2a_1}\left(\frac{K_2}{2p_1} - \frac{K_1^2}{8p_1^3} - p_3 - \frac{a_2K_1}{2a_1p_1} + \frac{a_2p_2}{a_1}\right)$,
$B_1 = \frac{1}{2a_1}(q_2 - \frac{L_2}{2\sqrt{L_1}})$, $B_2 = -\frac{1}{2a_1}(\frac{L_3}{2\sqrt{L_1}} - \frac{L_2^2}{8L_1^{3/2}} - \epsilon + \frac{a_2q_2}{a_1} - \frac{a_2L_2}{2a_1\sqrt{L_1}})$,
$C_1 = \frac{p_1}{a_1}$ $C_2 = \frac{1}{2a_1}(\frac{K_1}{2p_1} + p_2 - \frac{a_2p_1}{a_1})$,
$D_1 = \frac{q_1}{a_1}$, $D_2 = \frac{1}{2a_1}(q_2 + \frac{L_2}{2q_1} + \frac{2a_2q_1}{a_1})$,

Again by using the theorem of complex analysis as stated in section 3.5, we finally find the asymptotic expansion of the roots of equation (3.14) as

$$\gamma_1 \sim \frac{B_1}{2\sqrt{A_1}}\frac{1}{\omega}\left[1+\frac{1}{2B_1^2}\left\{A_2^2-2B_1B_2-\frac{\left(2A_1A_2+B_1^2\right)^2}{4A_1^2}\right\}\frac{1}{\omega^2}+o\left(\frac{1}{\omega^4}\right)\right] + i\sqrt{A_1}\left[1+\frac{4A_1A_2+B_1^2}{8A_1^2}\frac{1}{\omega^2}+o\left(\frac{1}{\omega^4}\right)\right] \tag{3.17}$$

$$\gamma_2 \backsim \omega\left[\sqrt{C_1}+\frac{4C_1C_2+D_1^2}{8C_1^{3/2}}\frac{1}{\omega^2}+o\left(\frac{1}{\omega^4}\right)\right] + i\frac{D_1}{2\sqrt{C_1}}[\left[1+\frac{1}{2D_1^2}\left\{C_2^2+2D_1D_2-\frac{\left(2C_1C_2+D_1^2\right)^2}{4C_1^2}\right\}\frac{1}{\omega^2}+o\left(\frac{1}{\omega^4}\right)\right] \tag{3.18}$$

3.6.3 Asymptotic results for different wave fields

In order to study the longitudinal plane waves in two modes in detail, we will now derive the expressions of the important wave components, like phase velocity, specific loss, penetration depth etc. of both the waves and examine these wave fields under the high frequency values.

(a). **Phase Velocity**

The phase velocity of wave is given by the formula

$$V_{E,T} = V_{1,2} = \frac{\omega}{\text{Real}(\gamma_{1,2})} \tag{3.19}$$

Where V_E and V_T denote the phase-velocities of elastic and thermal mode waves, respectively.

With the help of equations (3.17) and (3.18), and using the formula (3.19), we find the high frequency asymptotic expressions for V_E and V_T as follows:

$$V_E \sim \frac{1}{\sqrt{C_1}}\left\{1-\frac{4C_1C_2+D_1^2}{8C_1^2}\frac{1}{\omega^2}+o\left(\frac{1}{\omega^4}\right)\right\} \tag{3.20}$$

$$V_T \backsim \frac{2\sqrt{A1}}{B_1}\omega^2\left[1-\frac{1}{2B_1^2}\left\{A_2^2-2B_1B_2-\frac{\left(2A_1A_2+B_1^2\right)^2}{4A_1^2}\right\}\frac{1}{\omega^2}+o\left(\frac{1}{\omega^4}\right)\right] \tag{3.21}$$

***(b).* Specific Loss**

The ratio of energy dissipated per stress cycle to the total vibration energy is known as the specific loss, which is given as

$$SP_{E,T}=\frac{1}{4\pi}\left(\frac{\triangle W}{W}\right)_{1,2}=\frac{|\ \mathrm{Im}(\gamma_{1,2})\ |}{|\ \mathrm{Real}(\gamma_{1,2})\ |} \tag{3.22}$$

where $\left(\frac{\triangle W}{W}\right)_E$ and $\left(\frac{\triangle W}{W}\right)_T$ are the specific losses of elastic and thermal mode waves, respectively.

With the help of equations (3.17) and (3.18), and using this formula, we find the high frequency asymptotic expressions for SP_E and SP_T as follows:

$$SP_E\sim\frac{D_1}{2C_1}\frac{1}{\omega}\left[1-\frac{1}{2D_1^2}\left\{2D_1D_2-\frac{D_1^2+4C_1C_2D_1^2}{2C_1^2}\right\}\frac{1}{\omega^2}+o(\frac{1}{\omega^4})\right] \tag{3.23}$$

$$SP_T\sim\frac{A_1}{2B_1}\omega\Big[1+\frac{1}{2}\left\{\frac{4A_1A_2+B_1^2}{4A_1^2}-\frac{A_2^2-2B_1B_2}{B_1^2}+\frac{\left(2A_1A_2+B_1^2\right)^2}{4B_1^2A_1^2}\right\}\frac{1}{\omega^2}+o\left(\frac{1}{\omega^4}\right)\Big] \tag{3.24}$$

***(c).* Penetration Depth**

It is defined by the following relation

$$\delta_{E,T}=\delta_{1,2}=\frac{1}{|\ \mathrm{Im}(\gamma_{1,2})|} \tag{3.25}$$

where δ_E and δ_T are the penetration depths of elastic and thermal mode waves, respectively.

With the help of equations (3.17) and (3.18), we find the high frequency asymptotic expressions for δ_E and δ_T from the above formula as

$$\delta_E \sim \frac{2\sqrt{C_1}}{D_1}\left[1-\frac{1}{2D_1^2}\left\{2D_1D_2-\frac{D_1^2\left(D_1^2+4C_1C_2\right)}{4C_1^2}\right\}\frac{1}{\omega^2}+o\left(\frac{1}{\omega^4}\right)\right] \tag{3.26}$$

$$\delta_T \sim \frac{1}{\sqrt{A_1}}\left\{1-\frac{4A_1A_2+B_1^2}{8A_1^2}\frac{1}{\omega^2}+o(\frac{1}{\omega^4})\right\} \tag{3.27}$$

3.6.4 Case-II: Low frequency asymptotic expansions

For the low frequency asymptotic expressions of different wave fields, we use the similar approach as above and find the required roots of equation (3.14) by considering ω to be very very small, i.e., $\omega \ll 1$ and obtain the results as follows:

$$\begin{aligned}\gamma_1 \sim \sqrt{E_1}\omega\Bigg[&\left\{1+\frac{F_1^2-4E_1E_2}{8E_1^2}\omega^2+o(\omega^4)\right\}\\&+i\left\{\frac{F_1}{2E_1}\omega-\frac{8E_1^2F_2+F_1^3-4E_1E_2F_1}{16E_1^3}\omega^3+o(\omega^5)\right\}\Bigg]\end{aligned} \tag{3.28}$$

$$\gamma_2 \sim \sqrt{\frac{\epsilon}{2}}\sqrt{\omega}\left[\left\{1+\frac{G_1}{2\epsilon}\omega+o(\omega^2)\right\}+i\left\{1-\frac{G_1}{2\epsilon}\omega+o(\omega^2)\right\}\right] \tag{3.29}$$

where

$E_1=\frac{\left(-\sqrt{n_1}+p_3\right)}{2}$, $E_2=\frac{2a_2n_1-n_2+2p_2\sqrt{n_1}-2a_2p_3\sqrt{n_1}}{4\sqrt{n_1}}$, $F_1=\frac{1}{2}\left(\frac{m_1}{2\epsilon}+q_2\right)$,
$F_2=\frac{1}{2}\left\{\left(\frac{-m_1^2+4\epsilon^2m_2}{8\epsilon^3}+q_1\right)-a_2\left(\frac{m_1}{2\epsilon}+q_2\right)\right\}$, $G_1=\frac{1}{2}\left(\sqrt{n_1}+p_3\right)$,

and $n_1 = \frac{1}{2}\left(N_4 + \frac{M_4^2 - 2\epsilon^2 N_4}{2\epsilon^2}\right)$, $n_2 = \frac{1}{2}\left(N_3 - \frac{M_4^2 + 8\epsilon^6 N_3 - 4\epsilon^2 M_4^2 N_4 - 8\epsilon^4 M_3 M_4}{8\epsilon^6}\right)$,
$m_1 = \frac{1}{2}\left(-N_4 + \frac{M_4^2 - 2\epsilon^2 N_4}{2\epsilon^2}\right)$, $m_2 = -\frac{1}{2}\left(N_3 + \frac{M_4^2 + 8\epsilon^6 N_3 - 4\epsilon^2 M_4^2 N_4 - 8\epsilon^4 M_3 M_4}{8\epsilon^6}\right)$.

(a). **Phase Velocity**

In the similar way as followed in the previous case, we use formula (3.19) and equations (3.28) and (3.29) and find the low frequency asymptotic expressions for V_E and V_T as

$$V_E \sim \frac{\omega}{\text{Real}(\gamma_1)} = \frac{1}{\sqrt{E_1}}\left(1 - \frac{F_1^2 - 4E_1E_2}{8E_1^2}\omega^2 + o(\omega^4)\right) \tag{3.30}$$

$$V_T \sim \sqrt{\frac{2}{\epsilon}}\sqrt{\omega}\left(1 - \frac{G_1}{2\epsilon}\omega + o(\omega^2)\right) \tag{3.31}$$

(b). **Specific Loss**

With the help of equations (3.22), (3.28) and (3.29), we find the low frequency asymptotic expressions for SP_E and SP_T as

$$SP_E \sim \frac{F_1}{4E_1^2}\omega\left\{1 - \frac{3F_1^3 + 16E_1^2F_2 - 16E_1E_2F_1}{8E_1^2F_1}\omega^2 + o(\omega^4)\right\} \tag{3.32}$$

$$SP_T \sim 1 - \frac{G_1}{\epsilon}\omega + \frac{G_1^2}{2\epsilon^2}\omega^2 + o(\omega^3) \tag{3.33}$$

(c). **Penetration Depth**

Similarly, equations (3.25), (3.28) and (3.29) yield the low frequency asymptotic expressions for δ_E and δ_T in the forms

$$\delta_E \sim \frac{2\sqrt{E}_1}{F_1}\frac{1}{\omega^2}\left\{1 - \frac{4E_1E_2F_1 - 8E_1^2F_2 - F_1^3}{8E_1^2F_1}\omega^2 + o(\omega^4)\right\} \tag{3.34}$$

$$\delta_T \sim \sqrt{\frac{2}{\epsilon}}\frac{1}{\sqrt{\omega}}\left\{1 + \frac{G_1}{2\epsilon}\omega + o(\omega^2)\right\} \tag{3.35}$$

3.6.5 Amplitude coefficient factor and phase shift of thermodynamic temperature

From equations (3.5) and (3.11), $\theta(x,t)$ can be written as follows:

$$\theta(x,t) \;=\; BM\exp[i\Psi]\phi(x,t), \tag{3.36}$$

where $M,\ and\ \Psi$ are the amplitude coefficient factor and phase shift as compared to the conductive temperature, respectively and are given by

$$M = |1 + \alpha\gamma^2| \;\text{ and }\; \Psi = \text{Arg}(1 + \alpha\gamma^2) \tag{3.37}$$

Now, by expanding the expressions for M and Ψ from equation (3.37) and using equations (3.17), (3.18), (3.28) and (3.29), the asymptotic expressions for amplitude coefficient factor and phase-shift of the thermal mode waves for both high and low frequency values are derived as follows:

High frequency asymptotes:

$$M_T \approx 1 - \alpha A_1 \;\text{ as } \omega \to \infty \tag{3.38}$$

$$\Psi_T \approx -\pi + \frac{\alpha B_1}{\omega(1-\alpha A_1)} \quad \text{as} \quad \omega \to \infty \tag{3.39}$$

Low frequency asymptotes:

$$M_T \approx 1 + \frac{\alpha}{2}(2G_1 + \alpha\epsilon^2)\omega^2 \quad \text{as} \quad \omega \to 0 \tag{3.40}$$

$$\Psi_T \approx \alpha\epsilon\omega \quad \text{as} \quad \omega \to 0 \tag{3.41}$$

In the above expressions, the subscript T for M, and Ψ is used for thermal mode waves and we ignored the elastic wave component for this field as they lack physical meaning.

3.7 Numerical Results

In order to interpret the asymptotic results obtained in the previous section and to look into the nature of various wave components in details, we have made an attempt to find the numerical values of different wave characterizations for both the thermal and elastic mode longitudinal waves. To do this, we have assumed $h = 0.0168$, $\epsilon = 1.0168$, $\alpha = 0.071301$, $\tau_0 = 0.01$ *and* $\tau_1 = 0.02$. Using the software MATLAB, we have generated codes to compute the numerical values of different components directly from equation (3.13) and by using the formulas (3.19)-(3.21). The computation for the values of phase velocity, specific loss, penetration depth under all four cases TGL, TLS, GL and LS for different values of frequency, ω are carried out and the results are displayed in different Figures. In all

the Figures, we observe the variation of different wave characteristics with frequency in the contexts of four models. In Figs. (3.1)-(3.6), dashed lines colored with blue, red, magenta and cyan, are used to represent the profiles predicted by the two-temperature thermoelasticity models TGL and TLS and the generalized thermoelasticity models, GL and LS, respectively. In the next section, we will analyze our results and compare the numerical results with the analytical results.

3.8 Analysis of Analytical and Numerical Results

3.8.1 Phase velocity

The phase velocity of elastic and thermal mode longitudinal waves are displayed in Figs. 3.1(a,b) and 3.2(a,b), respectively. We observe from Figs. 3.1(a,b) that the two-temperature models (TLS and TGL models represented by red and blue colored dashed lines, respectively) predict significantly different results for the phase velocity of elastic mode wave as compared to the generalized theories (LS and GL models represented by cyan and magenta colored dashed lines, respectively). Furthermore, there is a significant difference between the results predicted by TLS and TGL models, but LS and GL do not show any prominent difference for this wave field. Our theoretical results indicate that $V_E \rightarrow$ constant limiting value as $\omega \rightarrow 0$ under TGL model and this is also in agreement with the numerical results (see Fig. 3.1(a)). Similar is the case with the other three models. However, this constant limiting value is dependent on the two temperature parameter as well as the two thermal relaxation parameters and are differ-

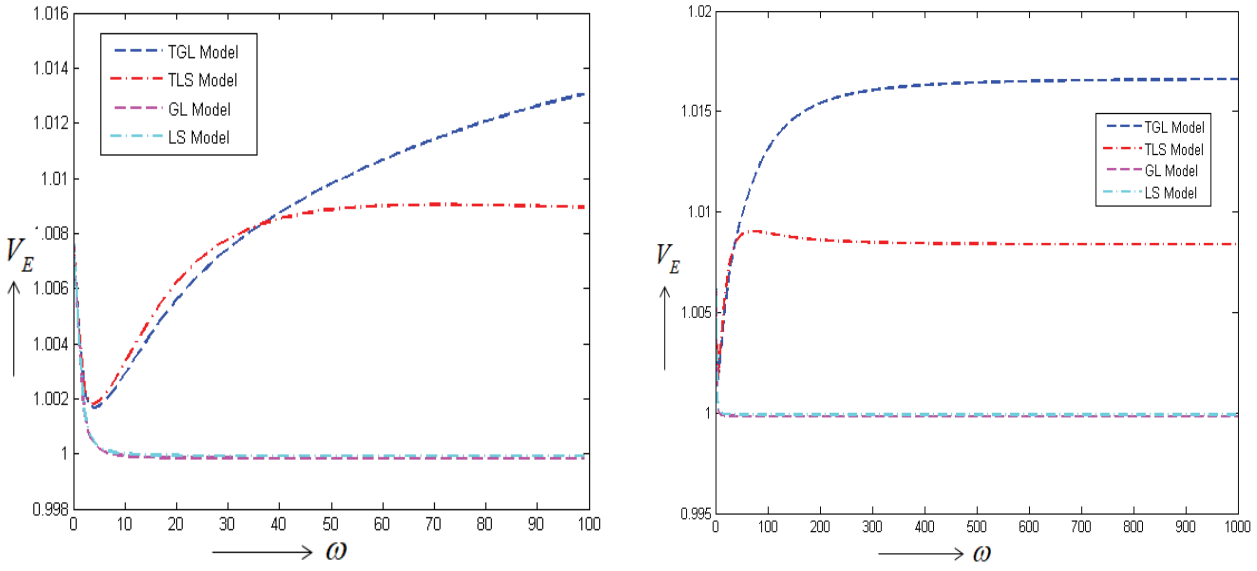

Figure 3.1: ***(a,b).*** Variation of the phase velocity, V_E of the elastic mode wave with frequency, ω

ent for TGL and TLS models, whereas they are the same for LS and GL models. Equation (3.20) as well as Fig. 3.1(b) suggest that $V_E \rightarrow$ constant value as $\omega \rightarrow \infty$ under TGL model. Similar behavior is observed for other models. However, the limiting values are significantly different under TLS, TGL models, although it is the same for LS and GL model. We further observe another important point : before reaching to the constant limiting value, the phase velocity of elastic mode wave shows a local minimum and a local maximum value under TLS model. The TGL model shows only one local minimum value and then slowly reaches to the constant limiting value as ω increases. LS model or GL model do not show any local minimum or maximum value.

Figs. 3.2(a,b) reveal that, as in the previous case, for the phase velocity of the thermal mode wave, the two-temperature models (TLS and TGL models represented by red and blue colored dashed lines, respectively) pre-

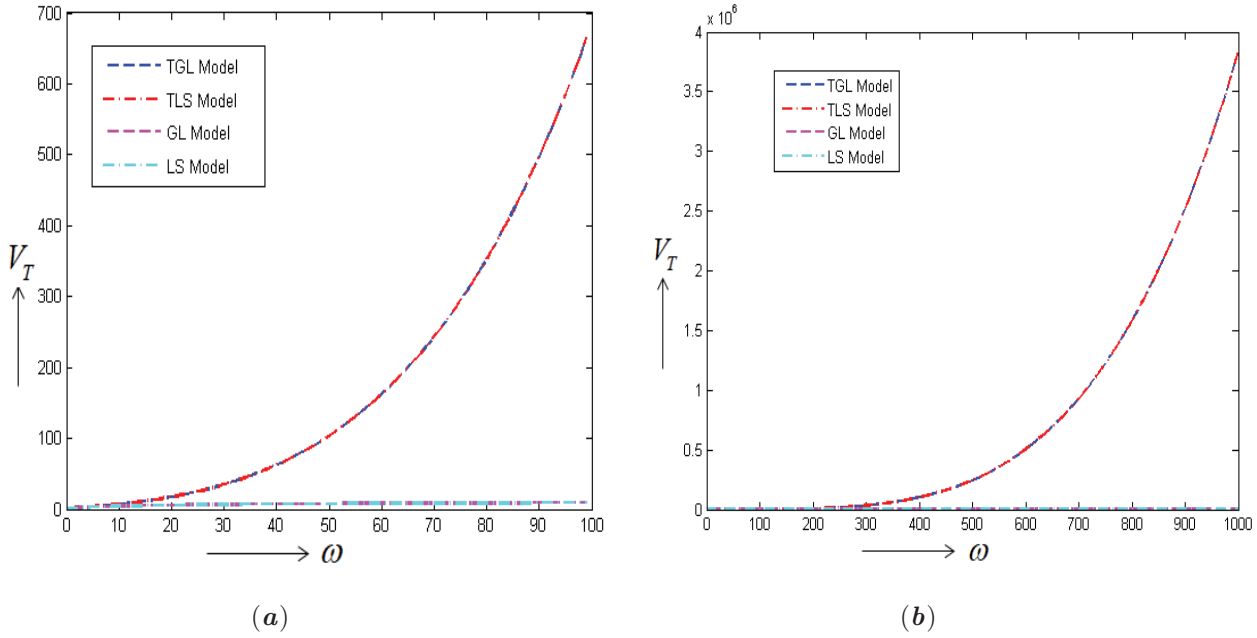

Figure 3.2: ***(a,b).*** Variation of the phase velocity, V_T of the thermal mode wave with frequency, ω

dict significantly different results as compared to the generalized theories (LS and GL models represented by cyan and magenta colored dashed lines, respectively). However, there is no prominent difference between the TLS and TGL models or between LS and GL models. $V_T \to 0$ as $\omega \to 0$ under all models. However, $V_T \to \infty$ as $\omega \to \infty$ under TGL as well as under TLS models. However, the LS model and GL model predict constant limiting value as $\omega \to \infty$. This fact verifies the fact that the generalized theories predict finite speed for thermal mode wave, but the two-temperature models do not predict the same and they also suffer from the physical drawback like classical Biot's model. This is indeed an important observation in the present study.

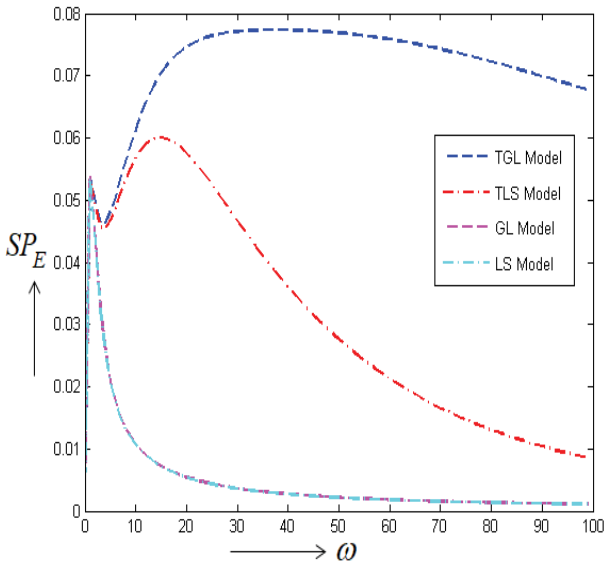

(*a*)

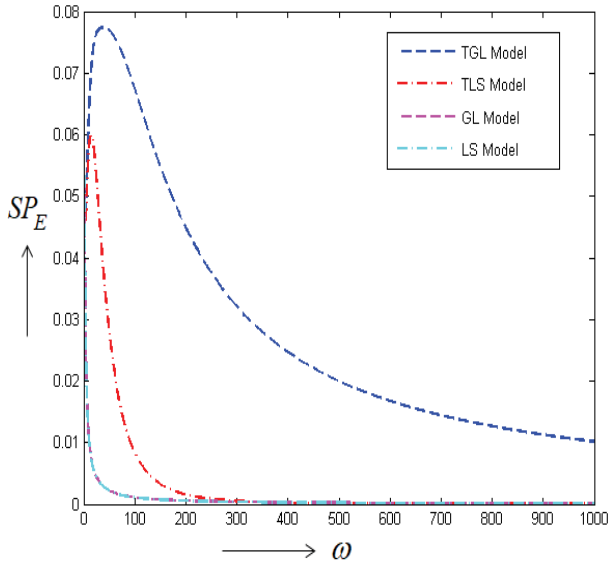

(*b*)

Figure 3.3: ***(a,b).*** Variation of the specific loss, SP_E of the elastic mode wave with frequency, ω

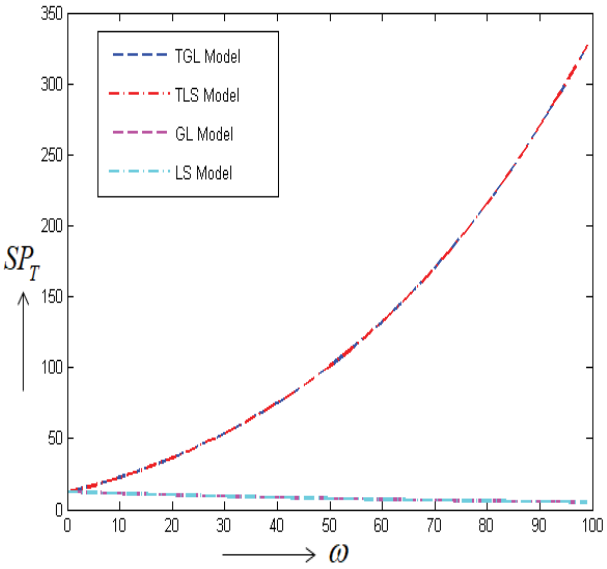

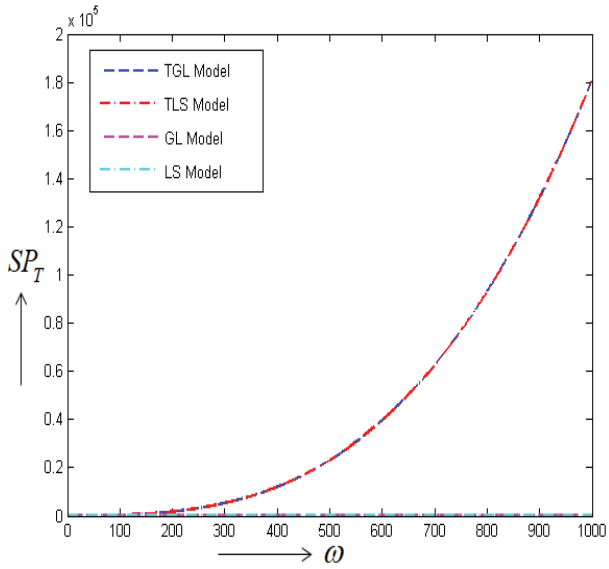

Figure 3.4: **(a,b).** Variation of the specific loss, SP_T of the thermal mode wave with frequency, ω.

3.8.2 Specific loss

Figs. 3.3(a,b) and 3.4(a,b) show the nature of variations of specific loss of elastic and thermal mode longitudinal waves, respectively. We see from Figs. 3.3(a,b) that there is no adequate difference in specific loss of generalized theories (LS and GL models represented by cyan and magenta colored dashed lines, respectively), but the two-temperature theories (TGL and TLS models represented by red and blue colored dashed lines, respectively) predict significantly different behavior as compared to generalized theories. $\left(\frac{\triangle W}{W}\right)_E \to 0$ as $\omega \to 0$ (see Fig. 3.3(a)) under all four cases which is in agreement with analytical result (see Equation (3.32)). Like phase velocity profiles, the specific loss behaves differently for generalized theories as compared to the two-temperature theories. This wave component achieves two local maximum values and one minimum value in the contexts of TLS and TGL models, but it shows only one local maximum in cases of LS and GL models. Further, we observe that under all four cases, specific loss finally tends to zero as $\omega \to \infty$ (see Fig 3.3(a)). However, it reaches to the limiting value zero much earlier in cases of LS and GL models and it reaches to zero under TGL model very slowly as compared to LS, GL and TLS models.

Specific loss of thermal mode longitudinal wave is displayed in Figs. 3.4(a,b). We observe from from Fig. 3.4(a) that $SP_T \to 1$ value as $\omega \to 0$ under all four cases which agree with the theoretical result (Eqn. (3.33) for TGL case). Specific loss of thermal wave also shows significantly different results under the generalized theories and the two-temperature theories.

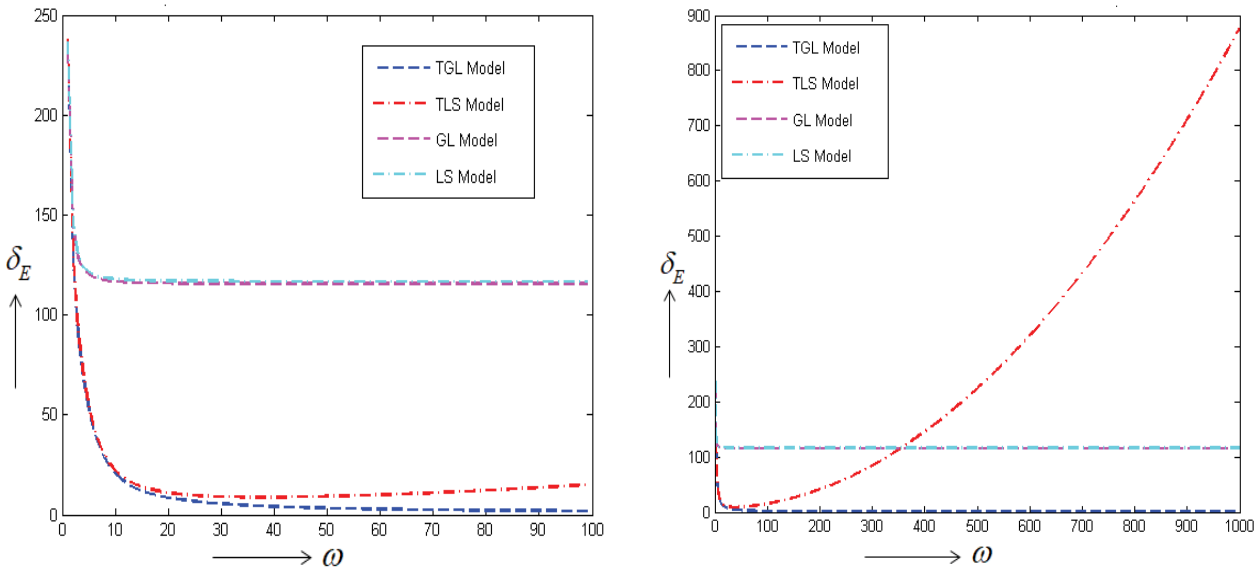

Figure 3.5: ***(a,b).*** Variation of the penetration depth, δ_E of the elastic mode wave with frequency, ω

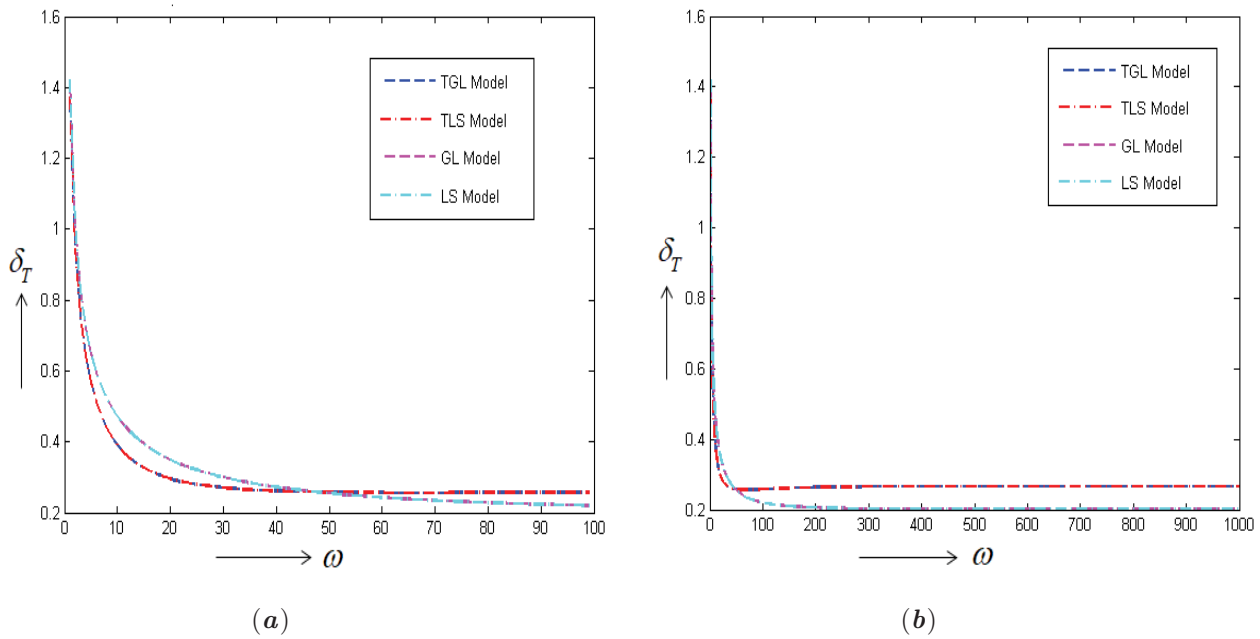

Figure 3.6: ***(a,b).*** Variation of the penetration depth, δ_T of the thermal mode wave with frequency, ω

However, specific loss does not predict prominently different results in the contexts of TGL and TLS models, or between GL and LS models. Equation (3.24) indicates that $\left(\frac{\triangle W}{W}\right)_T \to \infty$ as $\omega \to \infty$ for TGL model and this is in agreement with the numerical results (see Fig. 3.4(b) for TGL and TLS) which reveal that this field is an increasing function of frequency. This is also a significant difference predicted by the generalized and the two two-temperature theories. Our results in TLS model matches exactly with the corresponding results predicted by (Kumar and Mukhopadhyay, 2010b).

3.8.3 Penetration depth

Penetration depth of elastic and thermal mode longitudinal wave are depicted in Figs 3.5(a,b) and 3.6(a,b) respectively. From Figs. 3.5(a,b), we see that δ_E shows a prominent difference between generalized theories and two-temperature theories. Moreover, δ_E gives almost the similar results in the contexts of LS and GL models, but it shows significantly different values under the TLS and TGL models. We observe from Fig. 3.5(a) that $\delta_E \to \infty$ as $\omega \to 0$ in all four cases which is in agreement with theoretical result given by equation (3.34) (for TGL case). Theoretical result (see equation (3.26) for TGL model) as well as numerical results (Fig. 3.5(b)) reveal that $\delta_E \to$ constant limiting value as $\omega \to \infty$ under LS, GL and TGL models, but this limiting value depends on the two-temperature parameter significantly and are different for TGL and LS and GL models. This limiting value is nearer to 120 in cases of LS and GL models, but it is nearly 1 in case of TGL model. However, unlike these three models,

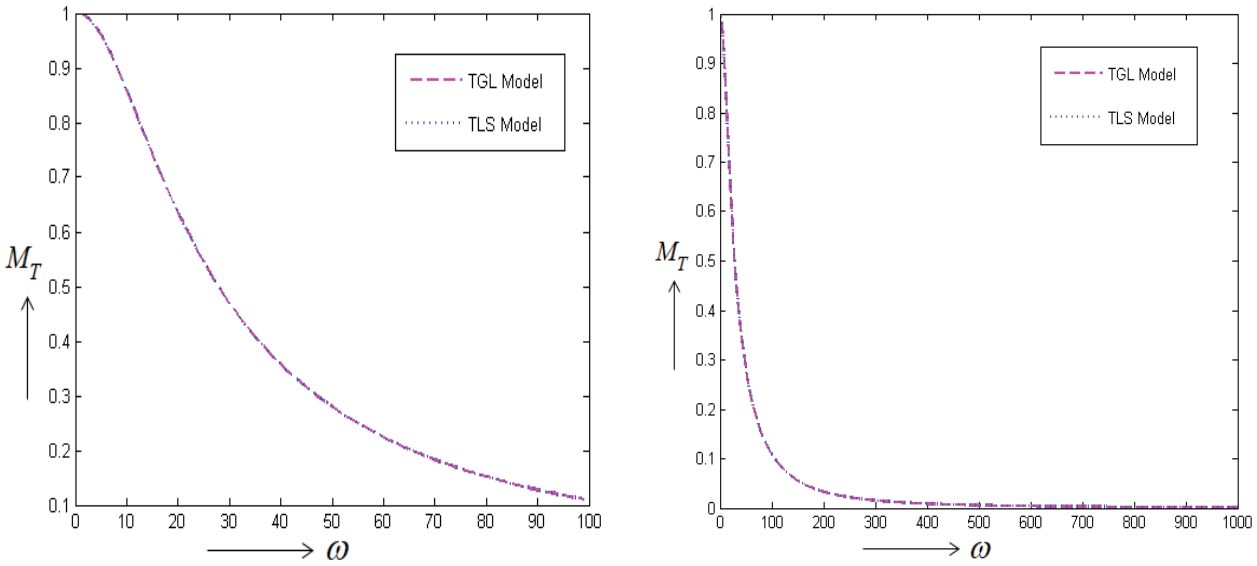

(*a*) (*b*)

Figure 3.7: ***(a,b).***Variation of the amplitude coefficient factor of the thermodynamic temperature, M_T for the thermal mode wave with frequency, ω

$\delta_E \to \infty$ as $\omega \to \infty$ in case of TLS model. This is an unrealistic feature of TLS model. This result is in complete agreement with the theoretical as well as numerical results predicted by Kumar and Mukhopadhyay (2010b).

The penetration depth for thermal mode wave is displayed in Figs. 3.6(a,b), from which it is clear that δ_E behaves differently in a significant manner under the generalized theories and the two-temperature theories. However, there is no prominent difference in the results shown by LS and GL models as well as under TGL and TLS models. From theoretical result (see equation (3.27)), $\delta_T \to$ constant as $\omega \to \infty$ for TLS and TGL models and $\delta_T \to 0$ as $\omega \to \infty$ in case of generalized theories (LS and GL models) which is in agreement with numerical results (see Fig. 3.6(b)). This indicates that the prediction of the two-temperature theories do not agree with the predictions of the generalized theories, although they all include thermal relaxation parameters.

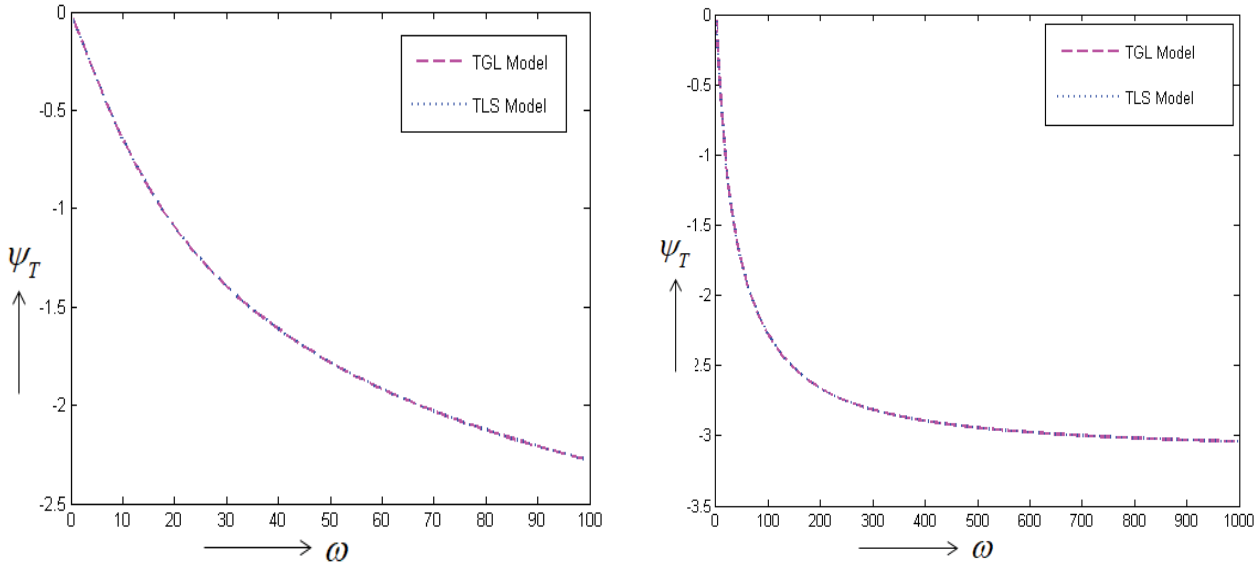

(*a*) (*b*)

Figure 3.8: ***(a,b).*** Variation of the phase shift, Ψ_T of the thermodynamic temperature for the thermal mode wave with frequency, ω

3.8.4 Amplitude coefficient factor and phase shift of thermodynamic temperature

The limiting behavior of the amplitude coefficient factor and the phase-shift of the thermodynamic temperature under TGL model can be observed from equations (3.37)-(3.40). The variations of these components with frequency are displayed in Figs. 3.7(a,b) and 3.8(a,b). From equations (3.38, 3.40), we note that the amplitude coefficient factor decreases with the increase of frequency and $|M_T B| \leq |B|$ i.e. the thermodynamic temperature exhibits a lesser magnitude as compared to the conductive temperature. This is also evident very clearly from Figs. 3.7(a,b). Furthermore, equations (3.39) and (3.41) indicate that as compared to the conductive temperature, the thermodynamic temperature experiences a phase shift $\Psi_T \leq 0$, where $\Psi_T \to 0 \,\text{as}\, \omega \to 0$ and $\Psi_T \to \text{constant}\,\text{as}\, \omega \to \infty$ (see Figs. 3.8(a,b) and also

Eqns. (3.39) and (3.41)). However, from Figs. 3.7(a,b) and 3.8(a,b), we note that TGL and TLS models predict similar results for both the fields.

3.9 Conclusions

In the present chapter, we investigate plane wave propagating in an unbounded thermoelastic medium. The dispersion relation solutions for the plane wave is derived by employing four different theories of thermoelasticity in order to investigate the effects of two thermal relaxation time parameters on plane harmonic wave under two-temperature theory. The asymptotic expressions for the important wave components like, phase velocity, specific loss, penetration depth etc. are derived for TGL model and we compare the results predicted by the corresponding results of TLS, LS and GL models. Variations of these wave components with frequency are investigated. Both the analytical and numerical results are found out and a detailed analysis is presented. Several important points regarding the predictions of various theories for the harmonic plane waves are highlighted. While doing our analysis of analytical and numerical results, we have found following remarkable results:

1. Although the transverse wave is unaffected due to the thermal field, but the longitudinal wave is coupled with the thermal field and there are two different modes of the longitudinal waves: one is pre-dominantly elastic and the other is pre-dominantly thermal in nature.

2. The predictions by the TGL and TLS models (two-temperature theories) are significantly different with the predictions by LS and GL models.

3. Under both the LS and GL models, the phase velocity of thermal mode

wave tends to a constant limiting value as the frequency increases, where as under the two-temperature theories the phase velocity of thermal wave increases with the increase of frequency and tends to infinity as frequency $\to \infty$. This is an unrealistic prediction by two-temperature theories like the classical coupled theory.

4. As a significant difference, the specific loss of thermal wave tends to infinity as $\omega \to \infty$ for TLS model, but this field tends to zero under TGL model. However, $\left(\frac{\triangle W}{W}\right)_T \to 0$ as $\omega \to \infty$ for GL and LS models. This is also a significant difference predicted by the generalized and the two-temperature theories including thermal relaxation parameters.

5. The penetration depth profile also shows a significant difference between the generalized theories and the two models of two-temperature theories. $\delta_T \to$ constant as $\omega \to \infty$ for TLS and TGL models but $\delta_T \to 0$ as $\omega \to \infty$ in case of generalized theories (LS and GL models). This is also an unrealistic feature predicted by the two-temperature models. Furthermore, there is a prominent difference between the results predicted by LS and GL, TLS and TGL models for the penetration depth for elastic wave. The trend is same for LS and GL models. $\delta_E \to$ constant as $\omega \to \infty$in both the cases. A similar nature is also observed in the context of TGL model, although the constant limiting value is nearer to 120 in cases of LS and GL models, and it is unity in case of TGL model. However, $\delta_E \to \infty$ as $\omega \to \infty$, which is an unrealistic prediction by TLS model and this feature is not observed in case of TGL model.

6. The models of two-temperature theories proposed by Youssef (2006b) includes thermal relaxation time parameters like the generalized theories

of thermoelasticity. However, they suffer the similar drawbacks like the classical theory. Furthermore, all the wave characteristics for both the waves show almost similar results in the contexts of LS and GL theories. However, the nature of wave components predicted by TGL and TLS models are significantly different and it is more prominent for the the wave characterizations of the elastic mode wave.